

Dithiophosphinate Complexes of Trivalent Lanthanide Cations: Consequences of Counterions and Coordination Number for Binding Energies and Selectivity. A Theoretical Study

Christian Boehme and Georges Wipff*

Laboratoire MSM, Institut de Chimie, UMR CNRS 7551, Université Louis Pasteur, 4 rue B. Pascal, 67 000 Strasbourg, France

Received August 9, 1999

Quantum-mechanical calculations are used to gain insight into the ligand–metal bonding in dithiophosphinate ($L = R_2PS_2^-$) complexes of trivalent lanthanides M^{3+} . The ligands are important in the context of liquid–liquid extraction of lanthanide(III) and actinide(III) ions from aqueous solutions. Our results demonstrate the importance of cumulative interactions and steric strain in the first coordination sphere of the metal. For the $[LM]^{2+}$ complexes, in the absence of competing ligands, phenyl-substituted ligands yield the highest binding energies and the order of metals is $La < Eu < Yb$. The sequence of the metal ligand interactions in 1:1 complexes is shown to differ from the order of the protonation energies of L. However, these results are strongly modulated if additional counterions or ligands are involved. In the $[LMCl_3]^-$ complexes alkyl-substituted ligands yield higher interaction energies than aryl-substituted ones, and generally the influence of the substituents R on the interaction energies becomes small. In the $[L_4M]^-$ complexes, the order of metals is reversed to $La > Eu > Yb$. The steric effect causing this reversal is stronger than all electronic effects of the substituents R on metal selectivity. The structures predicted at the Hartree–Fock level, under “gas-phase” conditions, are compared to structures predicted with correlated methods, with structures modeled in solution via the self-consistent reaction field (SCRF) method, and with experimental results.

1. Introduction

Organophosphorus ligands L are of great importance in the field of liquid–liquid extraction of lanthanide and actinide ions from aqueous solutions.^{1–3} The ligands used (see Figure 1) range from simple monodentate compounds such as TPPO and TBP to bidentate types such as CMPO and complex systems such as cavitands⁴ or the recently developed calixarenes,^{5–7} which utilize phosphoryl binding groups anchored to a lipophilic platform. While the mentioned ligands employ oxygen as a binding site, recently developed compounds such as the dithiophosphinic acid Cyanex 301^{8,9} show that sulfur can be a good alternative. The basic idea is that ligands based on sulfur, which is a “soft” base compared to oxygen, may not yield binding energies as high as oxygen-based ligands but may be more selective regarding cations of different sizes and “hardnesses”.

- (1) Rozen, A. M.; Krupnov, B. V. *Russ. Chem. Rev. (Engl. Transl.)* **1996**, 65, 973–1000 and references therein.
- (2) Choppin, G. R.; Nash, K. L. *Radiochim. Acta* **1995**, 70/71, 225–236.
- (3) Nash, K. L. *Solv. Extract. Ion Exch.* **1993**, 11, 729–768.
- (4) Boerrigter, H.; Verboom, W.; Reinhoudt, D. N. *J. Org. Chem.* **1997**, 62, 7148–7155.
- (5) Arnaud-Neu, F.; Böhmer, V.; Dozol, J.-F.; Grüttnner, C.; Jakobi, R. A.; Kraft, D.; Mauprivez, O.; Rouquette, H.; Schwing-Weill, M.-J.; Simon, N.; Vogt, W. *J. Chem. Soc., Perkin Trans. 2* **1996**, 1175–1182.
- (6) Barbosa, S.; Carrera, A. G.; Matthews, S. E.; Arnaud-Neu, F.; Böhmer, V.; Dozol, J.-F.; Rouquette, H.; Schwing-Weill, M.-J. *J. Chem. Soc., Perkin Trans. 2* **1999**, 719–723.
- (7) Delmau, L. H.; Simon, N.; Schwing-Weill, M.-J.; Arnaud-Neu, F.; Dozol, J.-F.; Eymard, S.; Tournois, B.; Böhmer, V.; Grüttnner, C.; Musigmann, C.; Tunayyar, A. *J. Chem. Soc., Chem. Commun.* **1998**, 1627–1628.
- (8) Zhu, Y. *Radiochim. Acta* **1995**, 68, 95–98. Zhu, Y.; Jiao, R. *Radiochim. Acta* **1995**, 69, 191–193.
- (9) Chen, J.; Zhu, Y.; Jiao, R. *Sep. Sci. Technol.* **1996**, 34, 2724–2731.

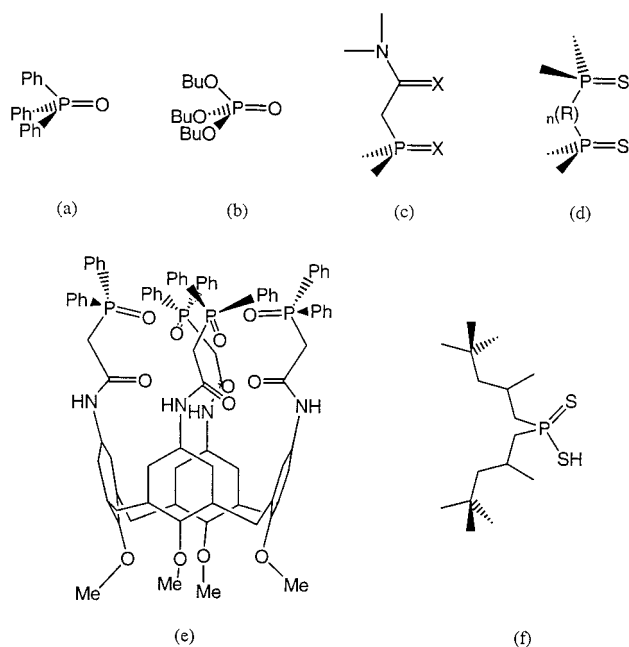


Figure 1. Typical phosphoryl-containing ligands of lanthanides and actinides: (a) TPPO; (b) TBP; (c) CMPO derivatives ($X = O$ or S); (d) dithiophosphine oxide; (e) calix[4]arene–CMPO derivative; (f) Cyanex 301.

The great amount of possible candidates makes choosing the right ligands for synthesis and testing as ligands in the liquid–liquid extraction of lanthanides and actinides very difficult. Experimental results obtained with ligands already tested can serve as a guideline, but a more general understanding of the

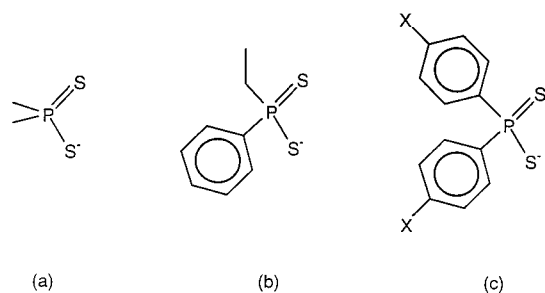


Figure 2. Calculated dithiophosphinic ligands L: (a) Me_2PS_2^- ; (b) PhEtPS_2^- ; (c) $(\text{XPh})_2\text{PS}_2^-$ ($\text{X} = \text{H}, \text{F}, \text{or } \text{NH}_2$).

different factors involved is desirable. In the case of the organophosphorus ligands, important factors are the binding site atom (oxygen or sulfur), the organic substituents on the phosphorus atom (e.g., aryls vs alkyls), the role of counterions, and the coordination number of the metal ion. In the absence of gas-phase data, quantum-mechanical calculations are an important source of information on these factors. This led our group to several theoretical studies on complexes of trivalent lanthanides with monodentate neutral phosphoryl^{10,11} (R_3PO) and thiophosphoryl¹² (R_3PS) ligands.

The results from these studies show that R_3PS ligands bind both more weakly and less selectively than the analogous R_3PO ligands to the different lanthanide cations tested (La^{3+} , Eu^{3+} , Yb^{3+}). In the 1:1 LM^{3+} complexes without counterions a strong aryl effect has been observed; i.e., ligands with aryl substituents R form considerably stronger bonds to the metal than those with alkyl substituents. This effect is strongly diminished in complexes with counterions; it is even reversed in the case of thiophosphoryl ligands. In all complexes with only one thiophosphoryl ligand, the small Yb^{3+} cation gives the highest binding energies, while in those with two thiophosphoryl ligands, the large La^{3+} cation is preferred, even though only by a very small margin.

In this study, we will extend our investigations to ligands L of the dithiophosphinate (R_2PS_2^-) type (see Figure 2). Such ligands have distinct advantages over the thiophosphoryl ligands we analyzed before. First, they carry a negative charge, which increases their donor capabilities, and second, they are bidentate, which furthermore improves their binding strength. One dithiophosphinate ligand studied experimentally, Cyanex 301^{8,9,13,14} (see Figure 1), has already been mentioned. Its performance in liquid–liquid extraction experiments is very promising. Modolo and Odoj have investigated dithiophosphinate ligands with different phenyl substituents, which showed increased extraction capabilities at low pH values, compared to Cyanex 301.¹⁵ They showed that electron-withdrawing substituents on the phenyl ring improve the extraction of Am(III) and of Eu(III), which is surprising, as such substituents decrease the donor strength of the ligand. The authors argue that the improved extraction is

an effect of the facilitated deprotonation of the ligands in acidic solution.

The first type of complexes reported here is the pure 1:1 form without counterions $[\text{R}_2\text{PS}_2\text{M}]^{2+}$. To assess the selectivity of the different ligands, La, Eu, and Yb are used as metals M, representing ions of different hardness from the large and therefore “soft” La^{3+} to the small and “hard” Yb^{3+} . The complexes without counterions allow us insight into the intrinsic properties of the dithiophosphinate–lanthanide complexes in the absence of external influences. Regarding the substituents R, the difference of aryl and alkyl is studied using phenyl and methyl as examples. Fluorophenyls, as studied experimentally,¹⁵ are discussed as well.

The influence of counterions is studied in complexes of the general formula $[\text{R}_2\text{PS}_2\text{MCl}_3]^-$. We chose to use negatively charged complexes of MCl_3 instead of neutral complexes of MCl_2^+ in order to obtain results comparable to those previously reported for the thiophosphoryl complexes R_3PSMCl_3 .¹² While the complexes formed in the extraction process are neutral, negatively charged dithiophosphinate–lanthanide complexes $[(\text{R}_2\text{PS}_2)_4\text{M}]^-$ are known from crystal structures (vide infra). Furthermore, the additional chloride anion provides for a higher coordination number in the studied complexes, which is therefore closer to the experimentally known coordination numbers of about 9. The metals M and the substituents R are the same as for the charged 1:1 complexes above, with the addition of an asymmetrically substituted ligand having ethyl and phenyl as substituents.

Finally, we report results for complexes of the general formulas $[(\text{Me}_2\text{PS}_2)_3\text{M}]$ and $[(\text{Me}_2\text{PS}_2)_4\text{M}]^-$, with M again being La, Eu, and Yb, which give insight into the changes in binding strengths and selectivities occurring when the coordination sphere of the metals becomes filled. Furthermore, these complexes allow for ligand–ligand interactions between dithiophosphinate ligands and can be compared to crystal structures obtained experimentally for $[(\text{R}_2\text{PS}_2)_4\text{M}]^-$ complexes.

While most of the calculations presented here were obtained at the Hartree–Fock (HF) level, correlation effects are studied in some cases using both second-order Møller–Plesset perturbation (MP2) and density functional theory (DFT). The influence of the liquid-phase environment on the structures of some of the studied ligands is investigated using the self-consistent reaction field (SCRf) method employing a simple cavity model. These influences are important for the understanding of the differences between the calculated and experimental structures.

2. Methods

The studied compounds were fully optimized at the Hartree–Fock level of theory. On sulfur, phosphorus, and carbon, the Dunning–Huzinaga double- ζ plus polarization basis sets¹⁶ were used. A basis set of the same type without a polarization function was used on hydrogen. A quasirelativistic ECP of the Stuttgart group^{17,18} was used on the lanthanides, together with the affiliated (5/4/3) valence basis.

For some compounds, SCRf (self-consistent reaction field) re-optimizations have been done in order to evaluate the influence of the solvent field on selected structures. The same level of theory as described above was used in these calculations. For the reaction field, the cavity model of Onsager^{19,20} was used with the dielectric constant

- (10) Troxler, L.; Dedieu, A.; Hutschka, F.; Wipff, G. *J. Mol. Struct. (THEOCHEM)* **1998**, *431*, 151–163. Bery, F.; Muzet, N.; Troxler, L.; Dedieu, A.; Wipff, G. *Inorg. Chem.* **1999**, *38*, 1244–1252. Baaden, M.; Bery, F.; Boehme, C.; Muzet, N.; Schurhammer, R.; Wipff, G. *J. Alloys Compd.*, in press.
- (11) Schurhammer, R.; Erhart, V.; Troxler, L.; Wipff, G. *J. Chem. Soc., Perkin Trans.* **1999**, 2515–2534.
- (12) Boehme, C.; Wipff, G. *J. Phys. Chem. A* **1999**, *103*, 6023–6029.
- (13) Jarvinen, G.; Barrans, R.; Schroeder, N. C.; Wade, K.; Jones, M.; Smith, B.; Mills, J.; Howard, G.; Freiser, H.; Muralidharan, S. In *Separations of Elements*; Nash, K. L., Choppin, G. R., Eds.; Plenum Press: New York, 1995; pp 43–62.
- (14) Hill, C.; Madic, C.; Baron, P.; Ozawa, M.; Tanaka, Y. *J. Alloys Compd.* **1998**, *271–273*, 159–162.
- (15) Modolo, G.; Odoj, R. *Solv. Extract. Ion Exch.* **1999**, *17*, 33–53.

- (16) Dunning, T. H.; Hay, P. J. In *Modern Theoretical Chemistry*. 3. Methods of electronic structure theory; Schaefer, H. F., III, Ed.; Plenum Press: New York, 1977; pp 1–28.
- (17) Dolg, M.; Stoll, H.; Savin, A.; Preuss, H. *Theor. Chim. Acta* **1993**, *85*, 441.
- (18) Dolg, M.; Stoll, H.; Savin, A.; Preuss, H. *Theor. Chim. Acta* **1989**, *75*, 173.
- (19) Onsager, L. *J. Am. Chem. Soc.* **1936**, *58*, 1486.

of tetrahydrofuran ($\epsilon = 7.58$). Other tests using the higher dielectric water ($\epsilon = 78.4$) as a continuum were also performed. To obtain an estimation of the influence of correlation effects, some compounds were studied using density functional theory at the local spin density approximation (LSDA) level, with gradient-corrected exchange and correlation functionals as derived by Becke²¹ and Perdew,²² respectively (BP86), and with the HF/LYP (Lee–Young–Parr) hybrid exchange functional (B3LYP²³). Additionally, one optimization with Møller–Plesset perturbation theory of the second order (MP2) has been performed.

The quantum chemistry program packages Gaussian 94²⁴ and Gaussian 98²⁵ were used throughout this study.

3. Results

We will first present the Hartree–Fock results, starting with the most simple complexes of the $[R_2PS_2M]^{2+}$ type. We will then proceed to the more complex systems of the $[R_2PS_2MCl_3]^-$ and finally the $[(Me_2PS_2)_3M]$ and $[(Me_2PS_2)_4M]^-$ types. An additional section discusses the changes occurring when the influences of electron correlation and the solvent are taken into account. The metal–ligand interaction energies can be found in Table 1 (see Figure 3 for the definitions); the most important structural features of the free ligands and the complexes are shown in Figures 4 and 5 and in Table 2. Mulliken charges are presented in Table 2, also.

3.1. The Charged 1:1 Complexes $[R_2PS_2M]^{2+}$: Importance of Substituent Effects to Intrinsic Metal–Ligand Interactions. The coordination of a negatively charged dithiophosphinate ligand $R_2PS_2^-$ to a “naked” Ln^{3+} cation leads to very high interaction energies, ranging from 490 to 560 kcal/mol, which for a large part result from the Coulombic interaction between the charged species. We did not calculate the dissociation energies for the dissociation in neutral ligands and M^{2+} (i.e., without charge separation), as we are mainly concerned with ligand exchange problems, but certainly the resulting energies would be lower.

In the process of coordination, charge is transferred from the ligand to the metal cation, which causes a change in the electronic structure of the ligand. This can be seen from the lengthening of the P–S bonds. In the free $Ph_2PS_2^-$ ligand, for example, the P–S bond lengths are 2.012 Å, and in the $[Ph_2PS_2Yb]^{2+}$ complex, they are 2.125 Å. This lengthening is consistent with the diminished charge difference between the P and S atoms. In the free ligand this difference is about 0.9

Table 1. Calculated Metal–Ligand Dissociation Energies ΔE and $\Delta E'$ (kcal/mol) from HF Calculations^a

| complex | ΔE | $\Delta\Delta E_L^b$ | $\Delta\Delta E_M^c$ |
|---|---------------------|----------------------|----------------------|
| Me ₂ PS ₂ H | −331.3 ^d | | 0.0 |
| Ph ₂ PS ₂ H | −323.8 ^d | | +7.5 |
| (FPh) ₂ PS ₂ H | −317.9 ^d | | +13.4 |
| Me ₂ PS ₂ La ²⁺ | −490.9 | 0.0 | 0.0 |
| Me ₂ PS ₂ Eu ²⁺ | −522.8 | −31.9 | 0.0 |
| Me ₂ PS ₂ Yb ²⁺ | −548.0 | −57.1 | 0.0 |
| Ph ₂ PS ₂ La ²⁺ | −498.5 | 0.0 | −7.6 |
| Ph ₂ PS ₂ Eu ²⁺ | −531.5 | −33.0 | −8.7 |
| Ph ₂ PS ₂ Yb ²⁺ | −563.7 | −65.2 | −15.7 |
| (FPh) ₂ PS ₂ La ²⁺ | −485.2 | 0.0 | +5.7 |
| (FPh) ₂ PS ₂ Eu ²⁺ | −517.9 | −32.7 | +4.9 |
| (FPh) ₂ PS ₂ Yb ²⁺ | −549.9 | −64.7 | −1.9 |
| Me ₂ PS ₂ LaCl ₃ [−] | −82.3 | 0.0 | 0.0 |
| Me ₂ PS ₂ SmCl ₃ [−] | −82.4 | −0.1 | |
| Me ₂ PS ₂ EuCl ₃ [−] | −82.4 | −0.1 | 0.0 |
| Me ₂ PS ₂ YbCl ₃ [−] | −81.0 | +1.3 | 0.0 |
| Ph ₂ PS ₂ LaCl ₃ [−] | −75.6 | 0.0 | +6.7 |
| Ph ₂ PS ₂ EuCl ₃ [−] | −75.6 | 0.0 | +6.8 |
| Ph ₂ PS ₂ YbCl ₃ [−] | −74.0 | +1.6 | +7.0 |
| (FPh) ₂ PS ₂ LaCl ₃ [−] | −72.5 | 0.0 | +9.8 |
| (FPh) ₂ PS ₂ EuCl ₃ [−] | −72.5 | 0.0 | +9.9 |
| (FPh) ₂ PS ₂ YbCl ₃ [−] | −71.0 | +1.5 | +10.0 |
| (H ₂ NPh) ₂ PS ₂ EuCl ₃ | −78.2 | | +4.2 |
| EtPhPS ₂ LaCl ₃ [−] | −84.0 | 0.0 | −1.7 |
| EtPhPS ₂ EuCl ₃ [−] | −79.4 | +4.6 | +3.0 |
| EtPhPS ₂ YbCl ₃ [−] | −82.5 | +1.5 | −1.5 |
| (Me ₂ PS ₂) ₃ La | +5.4 ^e | 0.0 | |
| (Me ₂ PS ₂) ₃ Eu | +5.0 ^e | −0.4 | |
| (Me ₂ PS ₂) ₃ Yb | +6.2 ^e | +1.2 | |
| (Me ₂ PS ₂) ₄ La [−] | −37.4 | 0.0 | |
| (Me ₂ PS ₂) ₄ Eu [−] | −29.0 | +8.4 | |
| (Me ₂ PS ₂) ₄ Yb [−] | −18.9 | +18.5 | |

^a See Figure 3 for definitions. ^b Difference in ΔE 's for a given ligand, relative to the lanthanum complex. ^c Difference in ΔE 's for a given metal, relative to the Me₂PS₂[−] complex. ^d Protonation energy of the R₂PS₂[−] ligand. ^e Reaction energy $\Delta E'$.

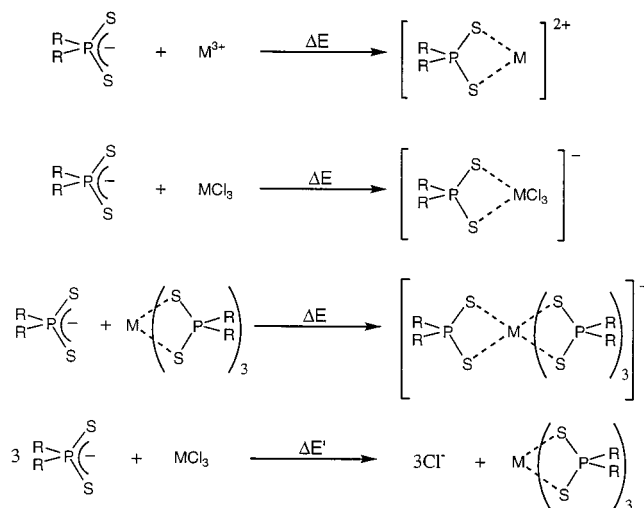


Figure 3. Definition of the calculated interaction energies ΔE and reaction energies $\Delta E'$.

e^- , according to the Mulliken charges. In the complex, charge is transferred from the sulfur atom to the Yb³⁺ cation, resulting in a charge difference between the P and S atoms of only about 0.5 e^- , which means less attraction between the two atoms.

It is informative to compare the charges obtained for the dithiophosphinate complexes with those obtained for the neutral thiophosphoryl (R₃PS) ones.¹² One difference is that the positive charge on the metal cation is much lower in the dithiophosphinate complexes (+1.6 to +1.9 e, compared to +2.1 to +2.4 e in the R₃PS complexes). This demonstrates the better donor

(20) Wong, M. W.; Wiberg, K. B.; Frisch, M. J. *J. Am. Chem. Soc.* **1992**, *114*, 1645.

(21) Becke, A. D. *Phys. Rev. A* **1988**, *38*, 3098.

(22) Perdew, J. P. *Phys. Rev. B* **1986**, *33*, 8822–8824.

(23) Becke, A. D. *J. Chem. Phys.* **1993**, *98*, 5648.

(24) Frisch, M. J.; Trucks, G. W.; Schlegel, H. B.; Gill, P. M. W.; Johnson, B. G.; Robb, M. A.; Cheeseman, J. R.; Keith, T.; Petersson, G. A.; Montgomery, J. A.; Raghavachari, K.; Al-Laham, M. A.; Zakrzewski, V. G.; Ortiz, J. V.; Foresman, J. B.; Peng, C. Y.; Ayala, P. Y.; Chen, W.; Wong, M. W.; Andres, J. L.; Replogle, E. S.; Gomperts, R.; Martin, R. L.; Fox, D. J.; Binkley, J. S.; Defrees, D. J.; Baker, J.; Stewart, J. P.; Head-Gordon, M.; Gonzales, C.; Pople, J. A. *Gaussian 94*, Revision B.2; Gaussian, Inc.: Pittsburgh, PA, 1995.

(25) Frisch, M. J.; Trucks, G. W.; Schlegel, H. B.; Scuseria, G. E.; Robb, M. A.; Cheeseman, J. R.; Zakrzewski, V. G.; Montgomery, J. A., Jr.; Stratmann, R. E.; Burant, J. C.; Dapprich, S.; Millam, J. M.; Daniels, A. D.; Kudin, K. N.; Strain, M. C.; Farkas, O.; Tomasi, J.; Barone, V.; Cossi, M.; Cammi, R.; Mennucci, B.; Pomelli, C.; Adamo, C.; Clifford, S.; Ochterski, J.; Petersson, G. A.; Ayala, P. Y.; Cui, Q.; Morokuma, K.; Malick, D. K.; Rabuck, A. D.; Raghavachari, K.; Foresman, J. B.; Cioslowski, J.; Ortiz, J. V.; Stefanov, B. B.; Liu, G.; Liashenko, A.; Piskorz, P.; Komaromi, I.; Gomperts, R.; Martin, R. L.; Fox, D. J.; Keith, T.; Al-Laham, M. A.; Peng, C. Y.; Nanayakkara, A.; Gonzalez, C.; Challacombe, M.; Gill, P. M. W.; Johnson, B.; Chen, W.; Wong, M. W.; Andres, J. L.; Gonzalez, C.; Head-Gordon, M.; Replogle, E. S.; Pople, J. A. *Gaussian 98*, Revision A.5; Gaussian, Inc.: Pittsburgh, PA, 1998.

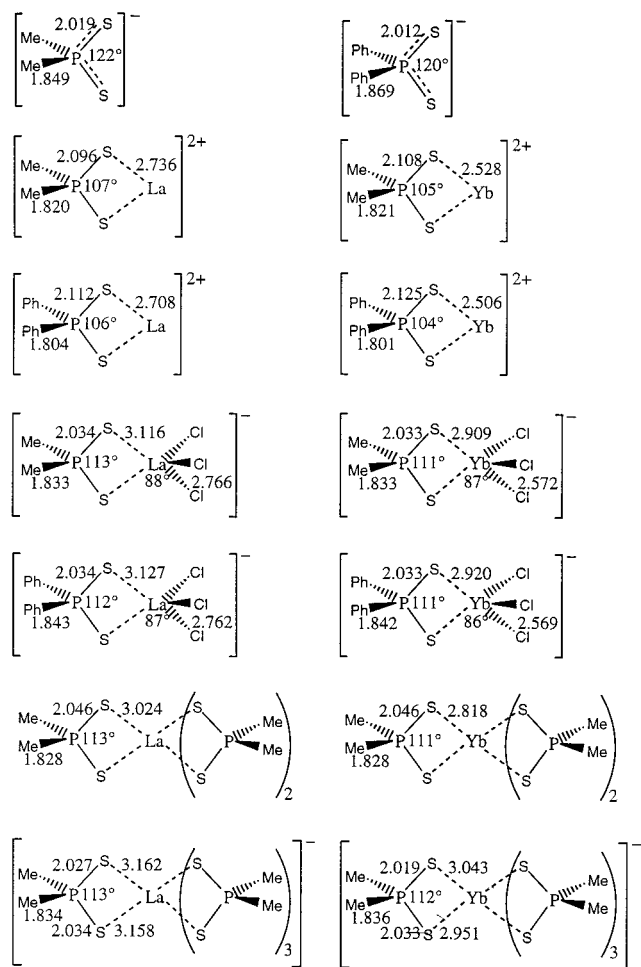


Figure 4. Optimized distances (Å) and angles in selected complexes.

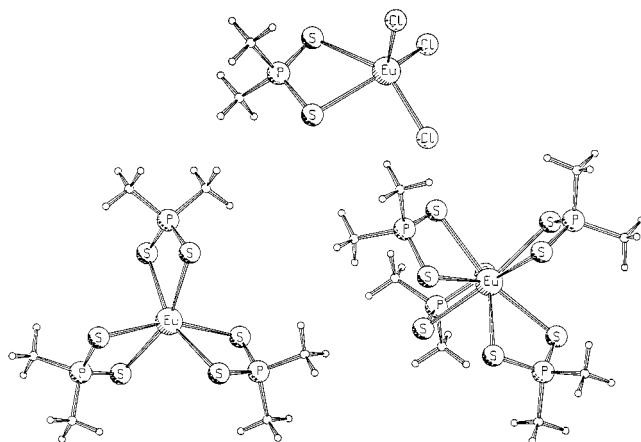


Figure 5. Ball and stick models of optimized complexes: $[\text{Me}_2\text{PS}_2\text{EuCl}_3]^-$, $(\text{Me}_2\text{PS}_2)_3\text{Eu}$, and $[(\text{Me}_2\text{PS}_2)_4\text{Eu}]^-$.

capabilities of the charged dithiophosphate ligands. Another clear distinction is the different behavior of the sulfur charges upon complexation. As seen above, the sulfur charges in the dithiophosphate ligands become lower due to the charge transferred to the metal. The sulfur charges in the thiophosphoryl complexes, on the other hand, become higher due to polarization of the ligand. This means that the binding of the R_3PS ligands is governed by ligand polarization, while the binding of the R_2PS_2^- ligands is governed by ligand–metal charge transfer.

The ligand–metal charge transfer is accomplished not only by removing electron density from the S atoms but also by removing it from the substituent R. This charge transfer is the

key to understanding the influence of the substituents R on the ligand–metal interaction energies ΔE . Phenyl is a larger and more polarizable substituent compared to methyl. According to the Mulliken charge analysis, it loses about $0.4 e^-$ upon complexation, while the methyl substituent loses only about $0.3 e^-$. Therefore the Ph_2PS_2^- ligand yields the stronger ligand–metal interaction with ytterbium, 20 kcal/mol more than that obtained with Me_2PS_2^- . *p*-Fluorophenyl is more electronegative and less polarizable than phenyl. Therefore the $\text{FPh}_2\text{PS}_2^-$ ligand yields ΔE 's which are about 15 kcal/mol smaller than those obtained with Ph_2PS_2^- . This result shows that the improved extraction capabilities of fluorophenyl-substituted dithiophosphate ligands, as they were reported by Modolo and Odoj,¹⁵ are not caused by enhanced metal–ligand interactions.

The interaction energies of the discussed ligands are strongly dependent on the cation size and “hardness”. The difference in ΔE 's, $\Delta\Delta E$, between the largest cation (La^{3+}) and the smallest one (Yb^{3+}) is about 60 kcal/mol for the three studied ligands. This is 1.5 times more than with the Ph_3PS ligand. The $\Delta\Delta E$'s follow the trend of the ΔE 's; i.e., the largest cation discrimination is observed with phenyl as the substituent. The substituent effect is small, however; the difference between phenyl and methyl in cation selectivity is only about 8 kcal/mol.

3.2. Noncorrelation of Protonation Energies of the Ligands with Metal–Ligand Interaction Energies in 1:1 Complexes.

The basicity of ligands is often assumed to be correlated to their donor strength.^{26–28} Indeed, we find that, among the phenyl-substituted ligands, the fluorophenyl derivative has a lower protonation energy and interacts less with the metals than the phenyl analogue (Table 1). That this correlation does not always hold is shown by the two ligands Me_2PS_2^- and Ph_2PS_2^- . According to our calculations, their gas-phase protonation energies are 331 and 324 kcal/mol, respectively. The phenyl-substituted Ph_2PS_2^- ligand has a lower basicity, but as shown above, it forms a stronger complex with the lanthanides than does the methyl-substituted one. Its lower basicity is caused by the good capability of the phenyl rings to delocalize and stabilize its negative charge. Its stronger interaction with trivalent cations, on the other hand, is explained by the better polarizability of the phenyl rings.

3.3. The $[\text{R}_2\text{PS}_2\text{MCl}_3]^-$ Complexes: Counterion Effects on Metal Ligand Interactions.

The addition of chloride counterions to the metal cations results in complexes which are closer to those expected in condensed phases, in terms of both metal cation charge and coordination number. It leads to a marked drop in the ligand-binding energy ΔE . In the case of Ph_2PS_2^- , for example, ΔE drops from 563.7 kcal/mol in $[\text{Ph}_2\text{PS}_2\text{Yb}]^{2+}$ to 74.0 kcal/mol in $[\text{Ph}_2\text{PS}_2\text{YbCl}_3]^-$. Upon the addition of counterions, the strong charge–charge interaction is substituted by a weaker charge–dipole interaction between the Ph_2PS_2^- and MCl_3 moieties. The charge transfer from the ligand to the metal is less pronounced in the complexes with counterions (according to the Mulliken charge $0.4 e^-$ in $[\text{Ph}_2\text{PS}_2\text{YbCl}_3]^-$ compared to $1.4 e^-$ in $[\text{Ph}_2\text{PS}_2\text{Yb}]^{2+}$), which in turn leads to a less pronounced elongation of the ligand's structure. For example the P–S bond elongation from the free to the complexed ligand is only 0.02 Å in $[\text{Ph}_2\text{PS}_2\text{YbCl}_3]^-$ compared to 0.11 Å in $[\text{Ph}_2\text{PS}_2\text{Yb}]^{2+}$. The charge difference between the P and S atoms is about $0.7 e^-$ with counterions, compared to $0.5 e^-$ without, in agreement with the diminished

(26) Martell, A. E.; Hancock, R. D. *Metal Complexes in Aqueous Solutions*; Plenum Press: New York, 1996; see also references therein.

(27) Hancock, R. D.; Martell, A. E. *Adv. Inorg. Chem.* **1995**, *42*, 89–146.

(28) Pearson, R. G. *Coord. Chem. Rev.* **1990**, *100*, 403–425.

Table 2. Selected Optimized Distances (r , Å) and Angles (α , deg) and Mulliken Charges q

| complex | method | r_{M-S} | r_{S-P} | r_{M-Cl} | α_{S-P-S} | α_{S-M-Cl} | $q(M)$ | $q(S)$ | $q(P)$ | $q(R)$ | $q(Cl)$ |
|---|---------------------------|-----------|-----------|------------|------------------|-------------------|--------|---------------------------|--------|--------|---------|
| Me ₂ PS ₂ ⁻ | HF/D95(d) | | 2.019 | | 122 | | | -0.64 | +0.54 | -0.13 | |
| Ph ₂ PS ₂ ⁻ | HF/D95(d) | | 2.012 | | 120 | | | -0.57 | +0.34 | -0.10 | |
| (FPh) ₂ PS ₂ ⁻ | HF/D95(d) | | 2.011 | | 121 | | | -0.56 | +0.35 | -0.11 | |
| (H ₂ NPh) ₂ PS ₂ ⁻ | HF/D95(d) | | 2.016 | | 120 | | | -0.59 | +0.34 | -0.09 | |
| Me ₂ PS ₂ H | HF/D95(d) | | 2.140 | | 114 | | | -0.41, -0.28 ^b | +0.45 | +0.01 | |
| Ph ₂ PS ₂ H | HF/D95(d) | | 2.143 | | 112 | | | -0.40, -0.25 ^b | +0.25 | +0.09 | |
| (FPh) ₂ PS ₂ H | HF/D95(d) | | 2.142 | | 113 | | | -0.40, -0.25 ^b | +0.25 | +0.08 | |
| Me ₂ PS ₂ La ²⁺ | HF/D95(d) | 2.736 | 2.096 | | 107 | | +1.88 | -0.35 | +0.42 | +0.20 | |
| Me ₂ PS ₂ Eu ²⁺ | HF/D95(d) | 2.625 | 2.102 | | 106 | | +1.74 | -0.29 | +0.42 | +0.21 | |
| Me ₂ PS ₂ Yb ²⁺ | HF/D95(d) | 2.528 | 2.108 | | 105 | | +1.64 | -0.24 | +0.41 | +0.22 | |
| Ph ₂ PS ₂ La ²⁺ | HF/D95(d) | 2.708 | 2.112 | | 106 | | +1.89 | -0.37 | +0.20 | +0.33 | |
| Ph ₂ PS ₂ Eu ²⁺ | HF/D95(d) | 2.599 | 2.119 | | 105 | | +1.75 | -0.31 | +0.19 | +0.34 | |
| Ph ₂ PS ₂ Yb ²⁺ | HF/D95(d) | 2.506 | 2.125 | | 104 | | +1.64 | -0.27 | +0.19 | +0.35 | |
| (FPh) ₂ PS ₂ La ²⁺ | HF/D95(d) | 2.712 | 2.111 | | 106 | | +1.90 | -0.37 | +0.20 | +0.33 | |
| (FPh) ₂ PS ₂ Eu ²⁺ | HF/D95(d) | 2.603 | 2.118 | | 105 | | +1.76 | -0.31 | +0.20 | +0.34 | |
| (FPh) ₂ PS ₂ Yb ²⁺ | HF/D95(d) | 2.509 | 2.125 | | 105 | | +1.65 | -0.27 | +0.19 | +0.35 | |
| Me ₂ PS ₂ EuCl ₂ | HF/D95(d) | 2.842 | 2.056 | 2.590 | 112 | 115 | +1.36 | -0.44 | +0.44 | +0.06 | -0.52 |
| Me ₂ PS ₂ LaCl ₃ ⁻ | HF/D95(d) | 3.116 | 2.034 | 2.766 | 113 | 88 | +1.38 | -0.49 | +0.46 | -0.02 | -0.61 |
| Me ₂ PS ₂ SmCl ₃ ⁻ | HF/D95(d) | 3.021 | 2.034 | 2.678 | 112 | 87 | +1.29 | -0.48 | +0.45 | -0.02 | -0.58 |
| Me ₂ PS ₂ EuCl ₃ ⁻ | HF/D95(d) | 3.005 | 2.034 | 2.663 | 112 | 87 | +1.27 | -0.48 | +0.45 | -0.02 | -0.58 |
| Me ₂ PS ₂ YbCl ₃ ⁻ | HF/D95(d) | 2.909 | 2.033 | 2.572 | 111 | 87 | +1.20 | -0.47 | +0.45 | -0.02 | -0.56 |
| Ph ₂ PS ₂ LaCl ₃ ⁻ | HF/D95(d) | 3.127 | 2.034 | 2.762 | 112 | 87 | +1.42 | -0.47 | +0.24 | +0.04 | -0.60 |
| Ph ₂ PS ₂ EuCl ₃ ⁻ | HF/D95(d) | 3.016 | 2.033 | 2.659 | 112 | 87 | +1.30 | -0.45 | +0.23 | +0.04 | -0.57 |
| Ph ₂ PS ₂ YbCl ₃ ⁻ | HF/D95(d) | 2.920 | 2.033 | 2.569 | 111 | 86 | +1.23 | -0.44 | +0.23 | +0.04 | -0.55 |
| (FPh) ₂ PS ₂ LaCl ₃ ⁻ | HF/D95(d) | 3.134 | 2.032 | 2.758 | 113 | 87 | +1.43 | -0.47 | +0.25 | +0.03 | -0.60 |
| (FPh) ₂ PS ₂ EuCl ₃ ⁻ | HF/D95(d) | 3.023 | 2.032 | 2.656 | 112 | 86 | +1.31 | -0.45 | +0.24 | +0.03 | -0.57 |
| (FPh) ₂ PS ₂ YbCl ₃ ⁻ | HF/D95(d) | 2.928 | 2.031 | 2.565 | 111 | 86 | +1.23 | -0.44 | +0.23 | +0.04 | -0.55 |
| (H ₂ NPh) ₂ PS ₂ EuCl ₃ | HF/D95(d) | 3.007 | 2.038 | 2.663 | 111 | 87 | +1.30 | -0.46 | +0.23 | +0.06 | -0.58 |
| (Me ₂ PS ₂) ₃ La | HF/D95(d) | 3.024 | 2.046 | | 113 | | +1.33 | -0.47 | +0.46 | +0.03 | |
| (Me ₂ PS ₂) ₃ Eu | HF/D95(d) | 2.914 | 2.046 | | 112 | | +1.25 | -0.46 | +0.45 | +0.02 | |
| (Me ₂ PS ₂) ₃ Yb | HF/D95(d) | 2.818 | 2.046 | | 111 | | +1.22 | -0.45 | +0.45 | +0.02 | |
| (Me ₂ PS ₂) ₄ La ⁻ | HF/D95(d) | 3.163 | 2.034 | | 113 | | +1.37 | -0.49 | +0.47 | -0.04 | |
| (Me ₂ PS ₂) ₄ Eu ⁻ | HF/D95(d) | 3.087 | 2.033 | | 113 | | +1.36 | -0.48 | +0.46 | -0.04 | |
| (Me ₂ PS ₂) ₄ Yb ⁻ | HF/D95(d) | 3.043 | 2.033 | | 112 | | +1.45 | -0.48 | +0.45 | -0.05 | |
| Me ₂ PS ₂ EuCl ₂ | SCRf(THF) | 2.813 | 2.066 | 2.610 | 111 | 117 | +1.33 | -0.44 | +0.45 | +0.09 | -0.54 |
| Me ₂ PS ₂ EuCl ₃ ⁻ | SCRf(THF) | 2.957 | 2.045 | 2.697 | 110 | 90 | +1.24 | -0.48 | +0.46 | +0.03 | -0.60 |
| Me ₂ PS ₂ EuCl ₃ ⁻ | SCRf(H ₂ O) | 2.943 | 2.049 | 2.708 | 110 | 90 | +1.23 | -0.48 | +0.46 | +0.04 | -0.60 |
| (Me ₂ PS ₂) ₃ Eu | SCRf(THF) | 2.914 | 2.046 | | 112 | | +1.25 | -0.46 | +0.45 | +0.02 | |
| (Me ₂ PS ₂) ₄ Eu ⁻ | SCRf(THF) | 3.087 | 2.033 | | 113 | | +1.36 | -0.48 | +0.46 | -0.04 | |
| Me ₂ PS ₂ Eu ²⁺ | BP86/D95(d) | 2.585 | 2.140 | | 107 | | +1.44 | -0.11 | +0.27 | +0.25 | |
| Me ₂ PS ₂ EuCl ₃ ⁻ | LSDA/D95(d) | 2.873 | 2.031 | 2.582 | 112 | 84 | +0.50 | -0.26 | +0.27 | -0.02 | -0.40 |
| Me ₂ PS ₂ EuCl ₃ ⁻ | LSDA/D95(d) ^a | 2.862 | 2.031 | 2.565 | 112 | 84 | +0.48 | -0.26 | +0.27 | -0.03 | -0.39 |
| Me ₂ PS ₂ EuCl ₃ ⁻ | BP86/D95(d) | 2.954 | 2.050 | 2.620 | 113 | 85 | +0.73 | -0.32 | +0.29 | -0.03 | -0.44 |
| Me ₂ PS ₂ EuCl ₃ ⁻ | BP86/D95(d) ^a | 2.946 | 2.050 | 2.605 | 113 | 85 | +0.72 | -0.32 | +0.29 | -0.03 | |
| Me ₂ PS ₂ EuCl ₃ ⁻ | B3LYP/D95(d) ^a | 2.963 | 2.045 | 2.612 | 113 | 86 | +0.82 | -0.36 | +0.37 | -0.04 | -0.46 |
| Me ₂ PS ₂ EuCl ₃ ⁻ | MP2/D95(d) ^a | 2.913 | 2.026 | 2.594 | 113 | 86 | +1.22 | -0.46 | +0.44 | -0.02 | -0.57 |
| (Me ₂ PS ₂) ₄ Eu ⁻ | LSDA/D95(d) | 2.918 | 2.034 | | 113 | | +0.15 | -0.24 | +0.29 | -0.05 | |
| (Me ₂ PS ₂) ₄ Eu ⁻ | BP86/D95(d) | 3.001 | 2.052 | | 113 | | +0.67 | -0.31 | +0.31 | -0.05 | |

^a With additional f orbitals on Eu. ^b Charge of the protonated sulfur atom.

P–S bond lengthening. The metal–sulfur bonds are longer by about 0.4 Å with counterions, also showing the weaker ligand–metal interaction.

In the [R₂PS₂MCl₃]⁻ complexes, the metal charges range from +1.20 to +1.42 e⁻. In the previously studied R₃PSMCl₃ complexes,¹² the metal charges range from +1.29 to +1.52 e⁻. This means that, in the complexes of the neutral R₃PS ligands, the loss of positive charge on the metal upon addition of counterions is much higher (about 0.9 e⁻) than in the complexes of the R₂PS₂⁻ ligands (about 0.4 e⁻), another sign of the good donor strength of the latter compared to the former.

The difference in the ligand–metal interactions caused by the addition of counterions also changes the influence of the substituents R, leading to reversed effects. The methyl-substituted ligand Me₂PS₂⁻ now yields a higher interaction energy than the phenyl-substituted ligand Ph₂PS₂⁻, in the case of ytterbium by 7 kcal/mol. The good polarizability of the phenyl ligand is less important here, which is also evident in the Mulliken analysis, which shows that the methyl and the phenyl

substituents both transfer about 0.1 e⁻ upon complexation, whereas the phenyl substituent transfers significantly more charge than the methyl substituent in the complexes without counterions. Furthermore, the phenyl ligand's binding energy is negatively influenced by phenyl–chloride repulsion. Substituting the phenyl groups with *p*-fluorophenyl groups shows the expected effect of lowering ΔE , but due to the lesser importance of substituent polarizability, the effect is only about 1–3 kcal/mol. Conversely, with *p*-aminophenyl substituents, the opposite result is obtained and ΔE is increased by about 3 kcal/mol. The asymmetrically substituted ligand EtPhPS₂⁻ with R₁ = ethyl and R₂ = phenyl yields ΔE 's close to those of the Me₂PS₂⁻ ligand.

Very interesting is the cation discrimination behavior in the [R₂PS₂MCl₃]⁻ complexes, where the large La³⁺ cation is bonded more strongly than the small Yb³⁺. The discrimination is very small, however, with $\Delta\Delta E$ being about 1–2 kcal/mol, which means that the addition of counterions to the first coordination sphere of the cations leads to an almost total loss

of cation selectivity. The results for the 4:1 complexes will shed some light on this surprising result.

3.4. The $(\text{Me}_2\text{PS}_2)_3\text{M}$ and $[(\text{Me}_2\text{PS}_2)_4\text{M}]^-$ Complexes: Increasing Steric Strain with High Coordination Numbers. To evaluate the impact of high coordination numbers and ligand–ligand interaction, we chose two types of complexes. First, we chose negatively charged 4:1 complexes $[(\text{R}_2\text{PS}_2)_4\text{M}]^-$. These are known from crystal structures, which allows us a comparison of experimental solid-state structures and theoretically predicted gas-phase structures. Second, we chose neutral 3:1 complexes $(\text{R}_2\text{PS}_2)_3\text{M}$, which are also known experimentally (see below). Their crystal structures show coordination of additional neutral ligands in most cases. They are especially relevant in the context of liquid–liquid extraction, as charge neutrality is required for the species to be extracted to an organic phase.

To avoid the problems of dissociation energies, which include a charge separation for the 3:1 complexes $(\text{Me}_2\text{PS}_2)_3\text{M}$, the energy $\Delta E'$ for exchanging three chloride anions for three Me_2PS_2^- anions is given (see Figure 3). A small amount (about 6 kcal/mol) of energy is required for this reaction, indicating that three chloride anions bind somewhat more strongly than three Me_2PS_2^- ligands to the cation. This is again nearly independent of the cation size, which means that cation discrimination is weak. As in the 1:1 complexes with counterions $[\text{R}_2\text{PS}_2\text{MCl}_3]^-$, the large lanthanum cation is slightly preferred over ytterbium by the R_2PS_2^- ligands (i.e., the chloride exchange requires a larger amount of energy with ytterbium). The structures of the 3:1 complexes show features that lie between those of the 1:1 complexes with and without counterions. In the ytterbium complexes of the Me_2PS_2^- ligand, the sulfur–metal bonds are 2.506 Å in the 1:1 complex without counterions, 2.909 Å in the 1:1 complex with counterions, and 2.818 Å in the 3:1 complex. The S–P bond lengths in the same complexes are 2.108, 2.033, and 2.046 Å, respectively. This order relates to the amount of charge transferred from each ligand to the metal cation, which becomes smaller with the number of competing ligands. According to the Mulliken analysis, the ligand–metal charge transfers per Me_2PS_2^- ligand are about 1.4 e^- in $[\text{Me}_2\text{PS}_2\text{Yb}]^{2+}$, 0.5 e^- in $[\text{Me}_2\text{PS}_2\text{YbCl}_3]^-$, and 0.6 e^- in $(\text{Me}_2\text{PS}_2)_3\text{-Yb}$.

The addition of a fourth Me_2PS_2^- ligand to the 3:1 complexes results in the negatively charged 4:1 complexes $[(\text{Me}_2\text{PS}_2)_4\text{M}]^-$. The energy of the interaction between the fourth ligand and the 3:1 complexes is smaller by at least 45 kcal/mol than the corresponding energy for the interaction of the same ligand with MCl_3 , indicating more ligand–ligand repulsions with the bidentate Me_2PS_2^- ligands than with the chloride anions. The addition also shows a strong cation discrimination of about 20 kcal/mol in favor of the large lanthanum compared to the ytterbium cation! These are again the results of ligand–ligand interactions, i.e., steric repulsion between the bidentate Me_2PS_2^- ligands, which becomes stronger in the complexes of the smaller cations. It should be noted that the discriminating effect is larger than any other in this study, which means that *steric effects in the first coordination sphere of the cation play a more important role in cation discrimination than any intrinsic properties of the ligand itself*.

The structures of the 4:1 $[(\text{Me}_2\text{PS}_2)_4\text{M}]^-$ complexes show sulfur–metal bond lengths which are larger by 0.04–0.14 Å compared to those of the 1:1 complexes $[\text{Me}_2\text{PS}_2\text{MCl}_3]^-$ with chloride counterions. The difference is larger in the ytterbium complexes, which is also a result of the strong steric repulsion between the ligands in the 4:1 complex of the relatively small

ytterbium cation. The S–P bond lengths are the same in both complex types. However, the per ligand charge transfer is smaller in the ytterbium 4:1 complex (about 0.4 e^-) than in $[\text{Me}_2\text{PS}_2\text{YbCl}_3]^-$ (about 0.5 e^-). It can still be concluded, though, that metal–ligand interactions are not the primary reason for the different interaction energies in 4:1 L_4M^- compared to LMCl_3 complexes.

3.5. Structures in Condensed Phases: Influence of the Solvent Field from SCRF Calculations. The precise structure of a compound may be perturbed when it is surrounded by a field caused by other molecules, i.e., in condensed phases. To obtain an estimation of this effect, we have performed self-consistent reaction field (SCRF) calculations of four selected compounds with THF as solvent (Table 2). The latter was chosen because its dielectric constant lies between that of water and typical organic solvents such as toluene, the two phases in liquid–liquid extraction experiments. For the small, asymmetrically substituted complexes $\text{Me}_2\text{PS}_2\text{EuCl}_2$ and $[\text{Me}_2\text{PS}_2\text{EuCl}_3]^-$, the results correspond to an increased sulfur–metal charge donation leading to a change of these compounds' dipole moments. The S–Eu bonds in these compounds shorten by about 0.05 Å, while the P–S bonds lengthen by about 0.01 Å, which shows the increased charge transfer from the sulfur to the metal atom, and presumably more effective metal–ligand interaction, compared to the case of the gas phase. With water as a solvent, these effects are slightly enhanced (Table 2). Similar metal–ligand bond shortening in the solvent field was also observed for water complexes of uranyl and plutonyl.²⁹ However, the medium effect on the Mulliken charges was small; charge differences were below 0.05 e^- . In the larger, symmetrically substituted complexes $(\text{Me}_2\text{PS}_2)_3\text{Eu}$ and $[(\text{Me}_2\text{PS}_2)_4\text{Eu}]^-$, the solvent field does not change the structure, as the charge transfer observed for the smaller compounds above would not lead to a change in the dipole moments of these species. The Mulliken charges in these complexes remain unchanged as well.

3.6. Effects of Electron Correlation on the Structures of the Complexes: DFT and MP2 Calculations. The influence of electron correlation on lanthanide complexes has been covered in our previous studies of phosphoryl^{11,12} and thiophosphoryl complexes.¹² While changes of the structures were found to be significant, the qualitative trends of the interaction energies ΔE did not change with the neutral ligands. This justifies our choice of the Hartree–Fock level for this study. However, as we also want to give an estimation of the quality of the theoretically predicted structures by comparing them to experimental X-ray structures, it is necessary to evaluate the influence of electron correlation on the predicted structures of the compounds covered in this study. This was achieved for the $[\text{Me}_2\text{PS}_2\text{EuCl}_3]^-$ and $[(\text{Me}_2\text{PS}_2)_4\text{Eu}]^-$ complexes (Table 2).

Using LSDA-DFT instead of HF leads to a pronounced shortening of the S–Eu bond by 0.13 Å in $[\text{Me}_2\text{PS}_2\text{EuCl}_3]^-$ and by 0.17 Å in $[(\text{Me}_2\text{PS}_2)_4\text{Eu}]^-$. The P–S bonds remain nearly unchanged, while the S–Eu–S angles become smaller by about 4°, also showing the increased S–Eu bond strength. If gradient corrections are introduced by using the BP86 functional, the S–Eu bond lengths are changed toward the HF values. With this functional, the S–Eu bond length differences between HF and DFT are only about 0.05 Å for $[\text{Me}_2\text{PS}_2\text{EuCl}_3]^-$ and 0.09 Å for $[(\text{Me}_2\text{PS}_2)_4\text{Eu}]^-$. The S–Eu–S angle is closer to the corresponding HF value as well. However, with BP86, one obtains longer phosphorus–sulfur bonds (by about 0.02 Å),

(29) Spencer, S.; Gagliardi, K.; Handy, N. C.; Ioannou, A. G.; Skylaris, C.-K.; Willetts, A.; Simper, A. M. *J. Phys. Chem. A* **1999**, *103*, 1831–1837.

Table 3. Experimental Structures

| REFCODE ^a | formula | (Ln-S) _{long} , Å | (Ln-S) _{short} , Å | ref |
|----------------------|---|----------------------------|-----------------------------|----------|
| CAXYIJ | ((PrO) ₂ PS ₂) ₃ (AcNMe ₂) ₂ La | 3.045 | 2.988 | <i>b</i> |
| DOJKUI | ((EtO) ₂ PS ₂) ₃ ((PhCH ₂) ₂ SO) ₂ La | 3.091 | 2.992 | <i>c</i> |
| DUWSET | ((PrO) ₂ PS ₂) ₃ (DMSO) ₂ La | 3.015 | 2.984 | <i>d</i> |
| ETPLAP10 | ((EtO) ₂ PS ₂) ₃ (Ph ₃ PO) ₂ La | 3.092 | 2.981 | <i>e</i> |
| ASTPSA | [((EtO) ₂ PS ₂) ₄ La] ⁻ | 3.013 | 2.958 | <i>f</i> |
| FEMJEM | [(Et ₂ PS ₂) ₄ La] ⁻ | 3.013 | 2.926 | <i>g</i> |
| CHTPSM10 | ((C ₆ H ₁₁) ₂ PS ₂) ₃ Sm | 2.795 | 2.781 | <i>h</i> |
| DUWSIX | [((PrO) ₂ PS ₂) ₂ (DMSO) ₃ Eu] ⁺ | 2.891 | 2.872 | <i>d</i> |
| DUWSIX | [((PrO) ₂ PS ₂) ₄ Eu] ⁻ | 2.912 | 2.872 | <i>d</i> |
| BIYYUD | [(Me ₂ PS ₂) ₄ Tm] ⁻ | 3.009 | 2.790 | <i>i</i> |
| DCHPLU10 | ((C ₆ H ₁₁) ₂ PS ₂) ₃ Lu | 2.698 | 2.681 | <i>j</i> |

^a Reference code of the Cambridge Structural Database (CSD). ^b Nagai, K.; Sato, Y.; Kondo, S.; Ouchi, A. *Bull. Chem. Soc. Jpn.* **1983**, *56*, 2605. ^c Imai, T.; Shimoi, M.; Ouchi, A. *Bull. Chem. Soc. Jpn.* **1986**, *59*, 669. ^d Imai, T.; Nakamura, M.; Nagai, K.; Ohki, Y.; Suzuki, Y.; Shimoi, M.; Ouchi, A. *Bull. Chem. Soc. Jpn.* **1986**, *59*, 2115. ^e Pinkerton, A. A.; Schwarzenbach, D. *J. Chem. Soc., Dalton Trans.* **1976**, 2466. ^f Pinkerton, A. A.; Schwarzenbach, D. *J. Chem. Soc., Dalton Trans.* **1981**, 1470. ^g Pinkerton, A. A.; Schwarzenbach, D.; Spiliadis, S. *Inorg. Chim. Acta* **1987**, *128*, 283. ^h Meseri, Y.; Pinkerton, A. A.; Chapuis, G. *J. Chem. Soc., Dalton Trans.* **1977**, 725. ⁱ Spiliadis, S.; Pinkerton, A. A.; Schwarzenbach, D. *J. Chem. Soc., Dalton Trans.* **1982**, 1809. ^j Pinkerton, A. A.; Schwarzenbach, D. *J. Chem. Soc., Dalton Trans.* **1980**, 1300.

compared to those obtained with both HF and LSDA. Adding HF exchange terms to DFT in the B3LYP functional, as expected, yields a structure slightly closer to the HF structure. Finally, with MP2, one obtains a S–Eu bond length for [Me₂PS₂EuCl₃]⁻ which lies between the LSDA and the BP86 values, 0.09 Å below the HF value. However, with MP2, the P–S bond length is *smaller* (by 0.008 Å) than it is without correlation, while with gradient-corrected DFT, it is *longer*.

3.7. Comparison of the Gas-Phase Predicted to Experimental Crystal Structures. In this section, we compare structural parameters predicted by our calculations to those observed in related X-ray structures. Strictly speaking, they should not be identical, as the former correspond to structures at rest in the gas phase, while in condensed phases the cation coordination number is higher (close to 9) and field and thermal effects may operate. Some experimental X-ray structures of dithiophosphinate lanthanide complexes with different metals can be found in Table 3. The lanthanum complexes fall roughly into two categories: first, neutral structures with three dithiophosphinate and two additional ligands, where the S–La bond lengths range from 2.981 to 3.092 Å; second, negatively charged structures with four dithiophosphinate ligands with somewhat shorter S–La bonds ranging from 2.926 to 3.013 Å. The latter can be compared to the [(Me₂PS₂)₄La]⁻ complex we calculated. At the HF level, S–La bond lengths from 3.158 to 3.162 Å were obtained, about 0.19 Å more than those in the experimental structures.

The europium complex [((PrO)₂PS₂)₄Eu]⁻ also has four dithiophosphinate ligands, but it should be noted that the latter are of the O–alkyl type instead of the alkyl substituents studied here. Its S–Eu bond lengths range from 2.872 to 2.912 Å. These can be compared to the same bond lengths in [(Me₂PS₂)₄Eu]⁻, for which the HF values range from 3.052 to 3.087 Å, again about 0.18 Å too long. Also of interest is the neutral 3:1 samarium complex ((C₆H₁₁)₂PS₂)₃Sm, as the Sm³⁺ radius is only about 0.02 Å larger than that of Eu³⁺.³⁰ Its S–Sm bond lengths range from 2.781 to 2.795 Å. The calculated S–Eu bond lengths in (Me₂PS₂)₃Eu are 2.914 Å. A test calculation on Me₂PS₂SmCl₃⁻ shows that calculated S–Sm bond lengths should be about 0.016 Å longer than those calculated for S–Eu. This means that the HF values for S–Eu bond lengths in (Me₂PS₂)₃Eu are too long by roughly 0.14 Å.

No experimental structures of ytterbium complexes comparable to the ones presented here are known to us. However, using a similar argument as for the samarium complex above, it can be estimated, from the thulium and lutetium complexes, that the sulfur–metal bond lengths calculated on the HF level are too long by roughly 0.13 Å for [(Me₂PS₂)₄Yb]⁻ and by roughly 0.11 Å for (Me₂PS₂)₃Yb.

For a given cation, the differences between calculated and experimental bond distances are only weakly affected by the number of ligands involved; i.e., differences of 3:1 vs 4:1 complexes are predicted correctly. However, the difference becomes smaller from lanthanum to ytterbium. This is probably a result of the large-core ECP's, which are more accurate for the heavier lanthanides, where the core electrons are bound more tightly to the metal. We want to point out, though, that our energy comparisons should not be affected by these problems, as all energy differences are calculated with the same metal on both sides of the equation (see Figure 2). As the approximations made in the metal description are the same in different configurations, the corresponding energy errors should vanish in the differences.

Regarding the correlated methods tested, it is interesting, that the sulfur–metal bond lengths calculated with the LSDA-DFT are in best agreement with the experimental values (Tables 2 and 3). Gradient-corrected DFT gives worse results for these bonds, and additionally the S–P bonds become somewhat too long as well. The computationally expensive MP2 method was not used for the larger complexes, but from the smaller test case, it can be concluded that it performs slightly less well than LSDA for the S–M bonds but better for S–P bonds and M–S–P angles, which means that altogether it gives the most accurate predicted structures.

4. Discussion and Conclusion

Our results show that dithiophosphinate ligands L (R₂PS₂⁻) give strong complexes with lanthanide(III) cations. Calculations with a progressive increase of the coordination number demonstrate the role of cumulative interactions on the effectiveness of metal–ligand binding. For the 1:1 complexes [LM]²⁺, the influence of the substituents R on the ligands L is quite large where ligands with aryl substituents R yield higher interaction energies than ligands with alkyl substituents. Para substitution on the aryl ligand also markedly modulates the interactions with the metal. If Cl⁻ counterions are taken into account in the [LMCl₃]⁻ complexes, this order is reversed, and the influence of R in these complexes becomes very small. In the [LM]²⁺

(30) Habenschuss, A.; Spedding, F. H. *J. Chem. Phys.* **1980**, *71*, 442–450.

complexes the interaction energies rise when the complexed metal becomes smaller, i.e., in the order $\text{La} < \text{Eu} < \text{Yb}$. In the $[\text{LMCl}_3]^-$ and L_3M complexes, this cation selectivity vanishes, and it is reversed in the $[\text{L}_4\text{M}]^-$ complexes, due to increased "steric repulsions" between the ligands, mostly of electrostatic origin. It has to be pointed out that the influence of this effect on metal selectivity is *stronger than that of any other effect encountered in this study*, which means that *steric interactions in the first coordination sphere may play a more important role in metal selectivity than the electronic effects of the substituents R*. This might be especially true if more bulky, bidentate counterions such as nitrates or carboxylates are added or if co-extractants such as tributyl phosphate (TBP) are used. Such interactions are likely to play a role also in the control of cation binding by dipicolinate type ligands.^{31,32}

It is clear from our results that the steric effects obtained for the $[\text{L}_4\text{M}]^-$ complexes are caused not by repulsions between the substituents R (R = methyl in our calculations, which means R is small) but by repulsions in the first coordination sphere of the metal. This offers an alternative explanation to the improvement of the extraction capabilities with fluorophenyl instead of phenyl as the substituent.¹⁵ With R = fluorophenyl, the donor strength of the R_2PS_2^- ligands is decreased, and therefore electron density is removed out of the first coordination sphere, thereby decreasing ligand–ligand repulsions. On the other hand, it is conceivable that the repulsions increase with R_2PO_2^- ligands, which bind closer to the metal than R_2PS_2^- ones and therefore cause more "crowding" in the first coordination sphere. A further effect of the steric repulsions in the first shell could be hindering of water coordination, which might improve extraction results.

Electrostatic strain induced by more remote negatively charged atoms of the ligands has been recently pointed out in a QM study on R_3PO complexes with lanthanide cations, where alkyl *vs* *O*-alkyl phosphoryl substituents were compared.¹¹ It was found that substituting Me_3PO by $(\text{MeO})_3\text{PO}$ leads to a reduction of interaction in 1:1 $\text{R}_3\text{PO}\cdot\text{M}^{3+}$ complexes, following a trend anticipated from the relative basicities of the ligands. The energy difference ΔE_{int} was small (about 2–3 kcal/mol). However, in the presence of counterions ($\text{R}_3\text{PO}\cdot\text{MCl}_3$ complexes), as well with higher stoichiometries (in $[\text{R}_3\text{PO}]_2 \text{MCl}_3$ complexes), the alkyl *vs* *O*-alkyl substituent effect was markedly amplified (ΔE_{int} was about 20 and 23–30 kcal/mol, respectively). This was attributed to the accumulation of negatively charged atoms around the cation in the complexes of $(\text{MeO})_3\text{PO}$. The latter repulse each other, leading to "steric strain" (mostly of electrostatic origin).

Another aspect of our study is the field effect of the surrounding medium on the complexes. In the SCRF formalism,

(31) Grenthe, I. *J. Am. Chem. Soc.* **1961**, *83*, 360–364.

(32) Renaud, F.; Piguet, C.; Bernardinelli, G.; Bünzli, J.-C. G.; Hopfgartner, G. *Chem.—Eur. J.* **1997**, *3*, 1646–1659.

the interaction energies cannot be directly determined from fragment calculations due to the different sizes of the corresponding cavities. However, changes in geometrical and electronic features suggest that unsymmetrical complexes are more stabilized (the metal–ligand bonds shorten and the charge transfer to the metal increases) than symmetrical ones by the surrounding dielectric. It can thus be speculated that asymmetry contributes to this stabilization. In this respect, we notice that, experimentally, cation extraction by dithiophosphinate ligands L takes place in synergistic mixtures involving other ligands such as TBP or TOPO,^{14,15} which lead to asymmetrical complexes.

In terms of ligand design for lanthanide or actinide separation, our study shows that effective metal–ligand interactions with dithiophosphinate type ligands are not solely determined by the intrinsic features of the metal and the ligand. Consideration of cumulative effects resulting from the combination of ligands and counterions is important to balance metal–ligand attractions against steric strain in the first coordination sphere and to monitor the effectiveness of substituent effects in these coordinated species. On the methodological side, our study also demonstrates how electronic effects (charge transfer, polarization, etc.) depend on the interplay between the metal–ligand interactions and interactions within the first shell. They can thus be hardly modeled with force field methods, unless comparisons are restricted to consistent series of complexes.^{33–37} It would thus be desirable to develop modeling techniques (e.g., mixed MM/QM approaches^{38–40}) which take these effects into account.⁴¹ Such methods might allow us to simulate complexation in condensed phases, where interactions beyond the first shell, solvation and dynamic features, contribute to the metal-binding selectivity.⁴²

Acknowledgment. The authors are grateful to the EU for research grants (F14W-CT98-5003 and F14WCT960022) and to the CNRS IDRIS and Université Louis Pasteur for allocation of computer resources.

IC990951H

- (33) Hay, B. P. *Coord. Chem. Rev.* **1993**, *126*, 177–236 and references therein.
- (34) Clement, O.; Rapko, B. M.; Hay, B. P. *Coord. Chem. Rev.* **1998**, *170*, 203–243.
- (35) Comba, P.; Gloe, K.; Inoue, K.; Krüger, T.; Stephan, H.; Yoshizuka, K. *Inorg. Chem.* **1998**, *37*, 3310–3315.
- (36) Comba, P. *Coord. Chem. Rev.* **1999**, *185–186*, 81–98 and references therein.
- (37) Hancock, R. D. *Acc. Chem. Res.* **1990**, *23*, 253–257.
- (38) Gao, J.; Freindorf, M. *J. Phys. Chem. A* **1997**, *101*, 3182–3188.
- (39) Thompson, M. A.; Glendening, E. D.; Feller, D. *J. Am. Chem. Soc.* **1994**, *116*, 10465–10476.
- (40) Tongraar, A.; Liedl, K. R.; Rode, B. M. *J. Phys. Chem. A* **1998**, *102*, 10340–10347.
- (41) Humbel, S.; Sieber, S.; Morokuma, K. *J. Chem. Phys.* **1996**, *105*, 1959.
- (42) Lehn, J. M. *Struct. Bonding* **1973**, *161*, 1–69.